Diffusivities of Macromolecules in Composite Hydrogels

Kimberly B. Kosto and William M. Deen
Dept. of Chemical Engineering, Massachusetts Institute of Technology, Cambridge, MA 02139

DOI 10.1002/aic.10216
Published online in Wiley InterScience (www.interscience.wiley.com).

Diffusivities of fluorescein-labeled macromolecules were measured in dilute aqueous solution (D_∞), agarose gels (D_a), and agarose–dextran composite gels (D) using fluorescence recovery after photobleaching. Macromolecules with Stokes–Einstein radii (r_s) ranging from 2.7 to 5.9 nm were used, including two globular proteins (ovalbumin and BSA) and three narrow fractions of Ficoll, a spherical polysaccharide. Gels with agarose volume fractions of 0.040 and 0.080 were studied with dextran volume fractions ranging from 0 to 0.0076 and 0 to 0.011, respectively. For both agarose concentrations, the Darcy permeability (κ) decreased by an order of magnitude as the dextran concentration in the gel was increased from zero to its maximum value. For a given gel composition, the relative diffusivity (D/D_∞) decreased as r_s increased, a hallmark of hindered diffusion. For a given test molecule, D/D_∞ was lowest in the most concentrated gels, as expected. As the dextran concentration was increased to its maximum value, two- to threefold decreases in relative diffusivity resulted for both agarose gel concentrations. The reductions in macromolecular diffusivities caused by incorporating various amounts of dextran into agarose gels could be predicted fairly accurately from the measured decreases in κ, using an effective medium model. This suggests that one might be able to predict diffusivity variations in complex, multicomponent hydrogels (such as those in body tissue) in the same manner, provided that values of κ can be obtained. © 2004 American Institute of Chemical Engineers *AIChE J,* 50: 2648–2658, 2004

Keywords: composite hydrogels, diffusivity, agarose, Ficoll, macromolecules, globular proteins, Darcy permeability, FRAP

Introduction

Hydrogels are materials in which a large volume of water is held within a crosslinked polymer network. They range in complexity from synthetic materials that contain a single polymer (such as polyacrylamide) to natural ones that are composites of several biopolymers. The current and potential uses of hydrogels in membrane and chromatographic separations, their increasing application in medical devices, and their occurrence in body tissues (such as basement membranes and cartilage) provide ample motivation for studying diffusion in such materials. For macromolecular solutes, in particular, a combination of steric and hydrodynamic effects causes diffusivities to be lower than those in water. That is, the crosslinked polymers prevent diffusing macromolecules from occupying certain positions and limit their possible paths. Further, by acting as fixed obstacles, the crosslinked polymers alter the fluid stresses, thereby increasing the drag coefficient for a solute molecule and decreasing its mobility. Both effects lower the measurable diffusivity of the macromolecular solute.

Macromolecular diffusivities in hydrogels have been measured using a variety of methods, including fluorescence recovery after photobleaching (FRAP) (Berk et al., 1993; Hou et al., 1990; Jain et al., 1990; Johnson et al., 1995; E. M. Johnson

W. M. Deen is also affiliated with the Biological Engineering Division, MIT, Cambridge MA 02139.
Correspondence concerning this article should be addressed to W. M. Deen at wmdeen@mit.edu.

et al., 1996; Moussaoui et al., 1992; Pluen et al., 1999; Saltzman et al., 1994; Wattenbarger et al., 1992), pulsed-field-gradient NMR (Gibbs et al., 1992), and holographic interferometry (Gong et al., 2000; Kosar and Phillips, 1995; Zhang et al., 1999). In general, the relative diffusivity (gel value divided by aqueous value) is found to decrease as molecular size and/or gel polymer concentration are increased. One way to describe the effects of molecular size is to use hindered transport theories developed for membranes with long, regularly shaped (such as cylindrical) pores (Deen, 1987). Thus, a given gel might be viewed as having a certain effective pore size and pore number density. However, there is no clear way to predict those pore parameters from actual compositional variables, such as the volume fraction of crosslinked polymer. Closer to reality are models that envision a gel as a network of polymeric fibers with fluid-filled interstices. In such models, it is usually assumed that a single type of rigid, cylindrical fiber is arranged in either a random or spatially periodic array (Amsden, 1998; Clague and Phillips, 1996; E. M. Johnson et al., 1996; Ogston, 1973; Phillips, 2000; Phillips et al., 1989, 1990). Although structurally more realistic, and sometimes quite accurate in predicting transport properties, the development of these models has been somewhat limited. The most complete fiber matrix models, that is, those that include mobility as well as steric effects (Clague and Phillips, 1996; E. M. Johnson et al., 1996; Phillips, 2000; Phillips et al., 1989, 1990), apply only to the simplest structures. In particular, fiber arrays with two or more different radii (that is, two-component gels) have been considered only in the context of water flow (Clague and Phillips, 1997). A major difficulty in modeling hindered diffusion or hindered convection is that hydrodynamic interactions in such systems are relatively long range. That is, the mobility of a diffusing macromolecule is affected by distant, as well as nearby, fibers. The need to consider many-body hydrodynamic interactions makes it challenging to model even one-component gels.

An alternative to detailed hydrodynamic models of fibrous membranes or gels is an "effective medium" approach, in which the structure of the material is accounted for indirectly by using a known value of the Darcy (or hydraulic) permeability (Brady, 1994; E. M. Johnson et al., 1996; Kapur et al., 1997; Kosar and Phillips, 1995; Phillips et al., 1989). In this type of model, the mobility of a diffusing macromolecule is related to the Darcy permeability by considering the drag on a sphere moving through a medium described by Brinkman's equation; larger Darcy permeabilities, which correspond to more open structures, yield greater mobilities. In principle, this way of linking diffusivities to water flow data might be useful for predicting or correlating diffusivities in complex, multicomponent gels, provided that the Darcy permeability can be measured. Such data are available for certain synthetic or biological gels (for example, Bolton et al., 1998; E. M. Johnson et al., 1996; Kapur et al., 1997; White and Deen, 2002).

For single-component, geometrically similar fibrous media (that is, same fiber volume fraction and type of fiber arrangement), it is well established that the Darcy permeability varies as the square of the fiber radius (Clague et al., 2000; Jackson and James, 1986). A consequence of this for fiber mixtures is that, for a system that consists initially of coarse fibers, adding even a small volume of fine fibers may greatly reduce the Darcy permeability (Clague and Phillips, 1997). This type of behavior was demonstrated recently in hydrogels by incorporating varying amounts of dextran ("fine fibers") into agarose gels ("coarse fibers") (White and Deen, 2002). In certain cases, the addition of modest amounts of dextran caused order-of-magnitude reductions in the measured Darcy permeability. Although developed mainly to mimic the transport properties of a biological material (glomerular basement membrane), the agarose–dextran composites also provide an opportunity to test the ability of the effective medium approach to predict diffusivities in hydrogels that are more complex than those often studied. In the work reported here, macromolecular diffusivities and Darcy permeabilities were measured in agarose–dextran composite gels of varying composition, and the utility of various models was examined.

Materials and Methods

Gel preparation

The gel synthesis procedure was similar to that used previously (White and Deen, 2002). Agarose (Type IV; Sigma, St. Louis, MO) was suspended in KCl-phosphate buffer (0.1 M KCl and 0.01 M sodium phosphate at pH 7.0) and heated in a 90°C oven for 4–6 h until it was completely dissolved. The hot agarose solution was poured carefully onto a 2.5-cm-diameter woven polyester support (catalog #148 248; Spectrum Laboratories, Rancho Dominguez, CA) that was placed on a heated glass plate. The mesh fibers in the support formed square openings of 43 μm and had a thickness of 70 μm, with 29% open area. After placing a second hot glass plate on top, the sample was cooled to room temperature and immersed in buffer overnight at 7°C. The gels to which dextran was to be added were immersed in 500 kDa dextran (Sigma) solutions of either 50 or 150 mg/mL for at least 24 h, which greatly exceeds the diffusional equilibration time calculated from reported diffusivities for dextran in agarose (Key and Sellen, 1982). A 2-Mrad exposure to an electron beam (High Voltage Research Laboratory at Massachusetts Institute of Technology) was used to covalently link the dextran to the agarose. After irradiation, each gel was equilibrated with a large volume of buffer (2 mL, as compared to a typical gel volume of 0.025 mL) to remove free dextran. The agarose concentrations of 4.1 and 8.2% (w/v) were converted to volume fractions (ϕ_a) by dividing by 1.025 (Johnson et al., 1995); that is, $\phi_a = 0.040$ or 0.080. The volume fractions of immobilized dextran (ϕ_d), determined as described below, ranged from 0.0008 to 0.011. Samples used for water filtration and diffusion measurements underwent identical treatment, except that the diffusion samples did not require a polyester support. For every filtration sample, a diffusion sample was made from the same batch of gel.

Gel dextran concentration

The concentration of dextran incorporated into a given agarose gel was obtained by determining both the equilibrium partition coefficient and the fraction immobilized by the electron beam. The partition coefficient (Φ) is the concentration of free dextran in an untreated gel (based on total gel volume) divided by that in the external solution, at equilibrium. The fraction of the free dextran in the gel that was subsequently immobilized is denoted as η. To measure those quantities, 1.5-cm-diameter disks were cut from agarose sheets prepared

Table 1. Properties of Test Molecules*

Macromolecule	M_W	D_∞ (10^{-7} cm^2/s) (monomer)	r_s (nm) Monomer	r_s (nm) Dimer	Dimer Fraction	Fluorescein Fraction
Ovalbumin	45,000	7.68 ± 0.17	2.8	4.1	0.05	<0.01
BSA	68,000	6.20 ± 0.12	3.5	5.0	0.16	0.05
Ficoll 21K	21,300	7.96 ± 0.35	2.7	—	<0.01	<0.01
Ficoll 61K	60,700	4.81 ± 0.09	4.5	—	<0.01	<0.01
Ficoll 105K	105,000	3.64 ± 0.05	5.9	—	<0.01	<0.01
DTAF	532	38.3 ± 1.4	0.6	—	—	—

*Diffusion coefficients, corrected to 20°C, are given as a mean ± standard error as detailed in the text. For the proteins and Ficolls, four to six samples were measured, whereas two samples were measured for DTAF.

as described above. The thickness of each sample was measured using a micrometer, with the gel placed between two microslides of known thickness, allowing its volume ($V_g \cong 0.03$ mL) to be determined. The gel samples were equilibrated first with a large volume (2.5 mL) of 50 or 150 mg/mL dextran solution. Some were then irradiated and some left untreated. After thorough rinsing, each was equilibrated with a large volume (2.5 mL) of buffer and the final dextran concentration in the solution determined using a phenol sulfuric acid assay (Dubois et al., 1956). The large volume of solution used in each equilibration (V_0) made the mass of dextran in the gel negligible in each case. Accordingly, mass balances for each step yield

$$\Phi = \frac{C_u V_0}{C_0 V_g} \tag{1}$$

$$\eta = 1 - \frac{C_t}{C_u} \tag{2}$$

where C_0 is the dextran concentration in the initial solution, C_u is the final concentration for untreated gels, and C_t is the final concentration for treated (irradiated) gels, each in mass units. It follows that the volume fraction of immobilized dextran is

$$\phi_d = \eta \Phi C_0 \hat{V}_d \tag{3}$$

where the specific volume of dextran is $\hat{V}_d = 0.61$ mL/g (Bohrer et al., 1979).

Darcy permeability

The Darcy permeability (κ) of each mesh-reinforced gel was measured as described previously (Johnson and Deen, 1996; Johnston and Deen, 1999; White and Deen, 2002). The gel membrane was placed in a 3-mL ultrafiltration cell (Millipore, Bedford, MA) that was filled with the KCl-phosphate buffer and pressurized to 20 kPa using nitrogen. Samples of filtrate collected over timed intervals were weighed to determine the volume flow rate (Q). The gel thickness (δ), measured by confining the membrane between two microscope slides of known thickness and using a micrometer, ranged from 70 to 140 μm. From these measurements, κ was calculated as

$$\kappa = \frac{\mu Q \delta}{\beta A \Delta P} \tag{4}$$

where μ is the viscosity of water, A is the exposed membrane area, ΔP is the pressure drop, and β is a correction factor that accounts for the increased flow resistance arising from the polyester mesh support. That factor, which increases with δ (Johnson and Deen, 1996), ranged from 0.36 to 0.60 in these experiments.

Test macromolecules

Fluorescein-labeled ovalbumin and BSA from Molecular Probes (Eugene, OR) were used without further purification. Narrow fractions of Ficoll were special-ordered from Pharmacia LKB (Piscataway, NJ). The three Ficoll fractions had weight-average molecular weights (M_W) of 21, 61, and 105 kDa. Based on information from the manufacturer, the polydispersity index (M_W/M_N, where M_N is number-average molecular weight) was 1.22, 1.15, and 1.13, respectively. The Ficolls were labeled using dichlorotryazinyl amino fluorescein (DTAF; Sigma) according to the method of De Belder and Granath (1973). The unreacted DTAF was removed using desalting chromatography columns (Bio-Rad, Hercules, CA) before the desired product was freeze-dried.

The properties of the five test macromolecules are given in Table 1. All diffusivities shown (D_∞) are those measured by us in bulk solution using FRAP, as discussed below. The Stokes–Einstein radius (r_s) for each major component was calculated from D_∞ using

$$r_s = \frac{k_B T}{6\pi\mu D_\infty} \tag{5}$$

where k_B is Boltzmann's constant and T is absolute temperature. Size-exclusion chromatography, using Superdex 200 (Pharmacia Biotech, Piscataway, NJ) and 0.1 M PBS at pH 7.4 as eluent, was used to estimate the fractional fluorescence attributable to either high or low molecular weight contaminants, which were interpreted as protein dimers or free fluorescein, respectively. The column was calibrated using macromolecules of known r_s, including four narrow fractions of Ficoll and a fluorescently labeled 2000-kDa dextran. The limit of detection for either dimers or free fluorescein was about 1%. Hence, entries of "<0.01" in Table 1 correspond to nondetectable contaminants. Dimers were present in both protein samples, most prominently with BSA (16% of total fluorescence). The values of r_s shown for the dimers in Table 1 were estimated from their column elution times. Free fluorescein was detectable only in the BSA sample. The effects of these impu-

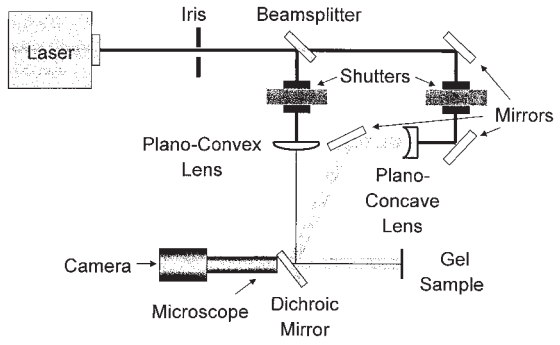

Figure 1. FRAP system used to measure diffusivities.

A 488-nm beam from an argon-ion laser was split into two beams, one of which was attenuated by a plano-concave lens and the other concentrated by a plano-convex lens. The 505-nm dichroic mirror reflected the 488-nm bleaching or attenuated laser beam onto the sample, while allowing the approximately 515-nm fluorescence emission to reach the camera.

rities on the diffusion measurements were generally small, as will be discussed. For ovalbumin and BSA, the r_s values for the monomers estimated from size-exclusion chromatography (3.1 and 3.7 nm, respectively) agreed well with those obtained using FRAP (Table 1). That was not true for a third protein, fluorescein-labeled IgG (from Jackson ImmunoResearch Laboratories, West Grove, PA). Chromatography of that IgG (M_W = 160 kDa) yielded a monomer radius of 4.7 nm, a dimer radius of 6.1 nm, a dimer fraction of 0.05, and a fluorescein fraction of <0.01. The FRAP data in free solution gave $D_\infty = (3.28 \pm 0.05) \times 10^{-7}$ cm^2/s, or a monomer r_s of 6.5 nm, larger even than that of the chromatographic dimer. Literature values of D_∞ for IgG (Burczak et al., 1994; Putnam, 1975) correspond to r_s = 5.4 to 5.6 nm. Because r_s could not be established unambiguously, experiments with IgG were discontinued.

FRAP diffusion experiments

Image-based FRAP (Berk et al., 1993; Tsay and Jacobson, 1991) was used to determine the diffusion coefficients of the test macromolecules in the gels and in bulk solution. The FRAP system assembled for this purpose is shown in Figure 1. An argon-ion laser (LS 300; American Laser, Salt Lake City, UT), emitting visible light at 488 nm in TEM00 mode, was used to irreversibly bleach the fluorescently labeled macromolecules. The laser light was split into two beams, one of which was attenuated by a plano-concave lens and the other concentrated by a plano-convex lens. By moving the latter, the diameter of the concentrated (bleaching) beam at the sample could be varied; that diameter was roughly 300 μm. Electronic shutters (Uniblitz, Rochester, NY), located in each beam path, controlled the type of illumination that reached the sample and the exposure time. A dichroic mirror (505 nm; Omega Optical, Brattleboro, VT) reflected the laser light onto the sample, but transmitted the fluorescent emission, which was imaged by a CCD camera (Cohu, San Diego, CA) fitted with a 4× microscope objective (N.A. 0.11) and a 15× eyepiece. Images, digitized using a frame grabber (IMAQ-PCI 1409; National Instruments, Austin, TX), could be taken at a maximum rate of 30 s^{-1}. A series of images taken at time steps ranging from 1 to 60 s, depending on the diffusivity of the macromolecule (that is, the timescale for fluorescence recovery), was analyzed to determine each diffusivity. At each time step, five images were taken in succession and averaged. From the original 640 × 780 pixels, a region 175 × 175 pixels centered on the bleached spot was saved for analysis. The spatial sampling rate, or distance between pixels, in either the horizontal or vertical direction was 3.8 μm, as measured by imaging a micrometer scale. The experiments were controlled and analysis done using Labview (National Instruments, Austin, TX) software. Diffusivities were measured at room temperature (22–28°C) and adjusted to 20°C by assuming that they vary as T/μ (Eq. 5).

Protein and Ficoll solutions were prepared by dissolving the test macromolecule in the KCl-phosphate buffer. The macromolecule concentrations ranged from 4 to 6 mg/mL, depending on the amount of fluorescence needed. The volume fraction of test macromolecules varied from 0.005 to 0.029, indicating that all solutions were dilute. To prepare for the FRAP measurements, the gel samples were first equilibrated with the fluorescent macromolecule solutions. The gels were then rinsed with buffer and placed between two glass slides with antireflection coatings (Edmund Industrial Optics, Barrington, NJ). Hematoseal (Fisher Scientific, Pittsburgh, PA) tube-sealing compound was applied to the edges to prevent evaporation. For a given solution or gel sample, measurements were repeated three times at different locations. Diffusion coefficients were measured for each macromolecule in four to eight gel samples with the same nominal agarose and dextran volume fractions. Gel and free-solution diffusivities were also determined for DTAF, which was assumed to be representative of any low molecular weight impurities.

FRAP data analysis

The diffusion coefficients were computed using spatial Fourier analysis of the digitized images (Berk et al., 1993; Johnson ME et al., 1996; Tsay and Jacobson, 1991). To allow for fluorescent impurities in the protein samples, as many as three components with differing diffusivities were considered. For three components, the transformed fluorescence intensity, relative to that before bleaching, is given by

$$f(t) \equiv \frac{\tilde{I}(u, v, t)}{\tilde{I}(u, v, 0)} = (1 - x_2 - x_3)\exp[-4\pi^2(u^2 + v^2)tD_1] + x_2\exp[-4\pi^2(u^2 + v^2)tD_2] + x_3\exp[-4\pi^2(u^2 + v^2)tD_3] \quad (6)$$

where x_i is the fraction of the fluorescence attributed to component i, D_i is the diffusivity of i, t is time, and u and v are spatial frequencies. The fluorescence fraction (x_i) is proportional to the number concentration of i times the fluorescence per molecule. Setting one or two of the fluorescence fractions to zero reduces Eq. 6 to the form used for two components or one component, respectively. For a specified number of components, the diffusivity data were fitted to Eq. 6 (or its analogs) using the Levenburg–Marquardt routine (Labview). A restriction that $f(t) \geq 0.38$ was applied to ensure that the edges of the Gaussian fluorescence profile were not cut off at any time during the fluorescence recovery (Berk et al., 1993). The eight lowest frequency pairs (u, v) following (0, 0), which produced similar recovery profiles with minimal noise, were the ones used to determine the diffusion coefficients. If the data from

any one frequency pair had an absolute mean square error that was at least twice the average for all pairs, it was discarded.

For measurements in free solution, each protein diffusivity (D_∞) was first calculated using the contaminant fractions obtained from size-exclusion chromatography (Table 1). So that the diffusivity of the predominant component (protein monomer) would be the only fitted parameter, D_∞ of the dimer was estimated from its chromatographic radius. The D_∞ of free fluorescein was assumed to equal that measured for DTAF (Table 1). Usually, a fit based on a single diffusing species was practically indistinguishable from ones that included two or three components. If the difference in D_∞ was $<2.5\%$, the single species fit was used. The exception was BSA, where D_∞ was calculated by including all three components detected by chromatography.

Steric exclusion of molecules by the gels during the initial equilibration with the test solution would have reduced the relative amounts of dimer in the gel and increased the relative amounts of free fluorescein. These effects would be greatest for the most concentrated gels. It follows that if dimer fractions were small enough to be neglected in free solution diffusivity measurements, then they could be safely neglected in analyzing any gel data. However, free fluorescein effects (if any) would be amplified. Thus, the quality of single-component fits to the FRAP data was expected to deteriorate as molecular size and/or gel concentration was increased. An example of this phenomenon is shown in Figure 2, in which fluorescence intensities for the largest Ficoll in 8.0% agarose are plotted as suggested by Eq. 6. In Figure 2a, which shows results both for pure agarose and for free solution, the single-component fits were excellent. However, in Figure 2b, which compares results for free solution with those for a more restrictive gel (dextran added to 8.0% agarose), the error in the single-component fit to the latter is unacceptable. As shown by the additional curve, the fit in Figure 2b was improved greatly by including free fluorescein as a second component, with the diffusivity of free fluorescein estimated from that measured for DTAF at that gel composition. The one additional degree of freedom in the two-component fit was the fractional fluorescence attributed to free fluorescein, which was found to be 0.12 in this case. In general, when free fluorescein had to be invoked in fitting the FRAP data, the fluorescence fractions obtained were <0.15. A free-fluorescein fraction of <0.01 in bulk solution (the limit of detection by chromatography) would become 0.15 in the gel if the partition coefficient of the test macromolecule were <0.067 times that of free fluorescein, which is quite reasonable for a concentrated gel. In other words, there was no inconsistency in fitting gel data with two components and free solution data with one component.

An analysis of the free solution data indicated that, in general, unbound fluorescein could be accurately distinguished (giving fluorescein fractions in accord with the chromatographic estimates) only if the macromolecule diffusivity was no more than 5% that of free fluorescein (as estimated using DTAF). When that criterion was met in a gel, a two-component fit (as in Figure 2b) was considered to be an acceptable way to reduce the error. Otherwise, one-component fits were generally used (as in Figure 2a), and usually exhibited no more error than that of two-component fits. In the exceptional case of BSA, where three components were needed to accurately fit the free solution data, the gel fits were also based on three components.

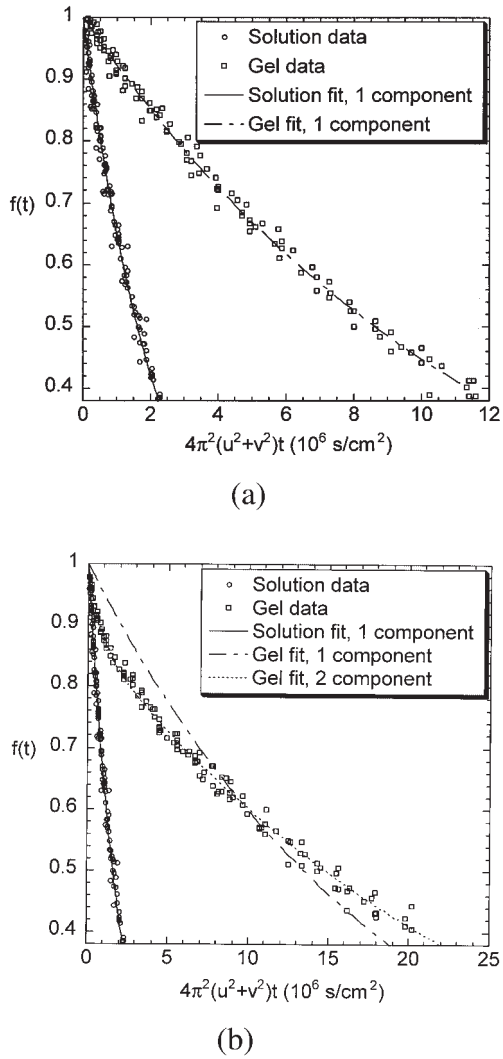

Figure 2. FRAP data for diffusion of 105 kDa Ficoll in buffer and in 8.0% agarose gels with or without dextran.

(a) Pure agarose ($\phi_a = 0.080$) and free solution. Both curves represent one-component fits. (b) Composite gel ($\phi_a = 0.080$ and $\phi_d = 0.011$) and free solution. One- and two-component fits to the gel data are shown, the latter being much more accurate.

In general, the variability between samples was larger than that among the three replicate measurements for each sample, so the standard error was computed based on the number of samples. When only two samples were examined, the error measure used was one-half of the difference between the two samples, plus the average standard error of the replicates.

Results

Gel composition

The six gel compositions used, designated A–F, are given in Table 2. The first two data columns (ϕ_a and ϕ_d) are the volume fractions of agarose and immobilized dextran, respectively. Two agarose volume fractions, $\phi_a = 0.040$ and 0.080, were each studied alone and with two levels of dextran. When present, dextran was the minority component, the highest value

Table 2. Properties of Composite Gels

Gel Type	ϕ_a	ϕ_d	C_0 (mg/mL)	Φ
A	0.040	0	0	—
B	0.040	0.0008**	50	0.39 ± 0.02*
C	0.040	0.0076 ± 0.0009	150	0.43 ± 0.02*
D	0.080	0	0	—
E	0.080	0.0008 ± 0.0004	50	0.24 ± 0.01
F	0.080	0.0110 ± 0.0005	150	0.38 ± 0.01*

ϕ_d and Φ are given as mean ± standard error for eight samples.
*These values were not statistically different, as determined by Tukey's method of multiple comparisons (Larson and Marx, 1986).
**Interpolated, assuming that η was proportional to C_0 (see text).

of ϕ_d being 0.011 (gel type F). The fraction of dextran immobilized (η, not shown) was found to increase with the dextran concentration in the initial equilibrating solution (C_0), reaching maximum values of 0.20 and 0.32 in 4.0 and 8.0% agarose, respectively. For gel type B, the results for η at the lower dextran concentration showed excessive variability, so that, to calculate ϕ_d for this case, η was estimated by linear interpolation in C_0. (It was found that η was a linear function of C_0 in 8.0% agarose.) Also shown in Table 2 are the values of C_0 and the partition coefficient measured for free dextran (Φ). As expected theoretically (White and Deen, 2001), Φ tended to decrease with increasing ϕ_a (for fixed C_0) and tended to increase with increasing C_0 (for fixed ϕ_a), although the differences were not always statistically significant.

It should be mentioned that the values of ϕ_d in Table 2 are roughly half those reported by White and Deen (2002) for similar gels. In that study, fluoresceinated dextran was used to determine η and ϕ_d. However, we noticed subsequently that such dextran solutions became gelatinous after electron beam irradiation, whereas unlabeled dextran was visibly unchanged. Accordingly, we used only unlabeled dextran here. Because the solutions used to determine ϕ_d were identical to those used to prepare the gel samples for permeability and diffusivity measurements, the present estimates of gel dextran content should be more reliable.

Diffusion in free solution

The diffusivities obtained for the proteins and Ficolls in free solution (D_∞) are given in Table 1. The present values for ovalbumin and BSA are each near the middle of the respective ranges in the literature. Those ranges, as summarized by Johnson et al. (1995), are 7.2×10^{-7} to 7.9×10^{-7} cm^2/s for ovalbumin and 5.8×10^{-7} to 6.4×10^{-7} cm^2/s for BSA. Accordingly, the values of molecular radius (r_s) for ovalbumin and BSA, which were calculated from D_∞ using Eq. 5, are also consistent with previous reports. Likewise, r_s for the Ficoll fractions was within 0.2–9.5% of measurements with corresponding unlabeled samples using quasi-elastic light scattering (Oliver et al., 1992).

Diffusion in agarose

Relative diffusivities in pure agarose gels are plotted as a function of molecular radius in Figure 3. The relative diffusivity is the diffusivity in the gel (D) divided by that in free solution (D_∞). Results are shown for 4.0% agarose (Figure 3a) and 8.0% agarose (Figure 3b). In each case, the present results for irradiated agarose (open symbols) are compared with previous data for untreated gels of approximately the same concentration (filled symbols; E. M. Johnson et al., 1996). The protein and Ficoll diffusivities generally followed the same decreasing trend as molecular size was increased. The relative diffusivities in the irradiated gels decreased from about 0.7 to 0.5 in 4.0% agarose and from about 0.4 to 0.2 in 8.0% agarose, as the molecular radius increased from 2.7 to 5.9 nm. Although the results overlapped, the values for irradiated gels tended to be slightly higher than those in untreated gels. Because the agarose concentrations in the previous untreated gels were somewhat lower than those in the present study (0.038 vs. 0.040, and 0.073 vs. 0.080), the actual effect of irradiation was somewhat greater than implied by the plots. Nonetheless, the increase in macromolecular diffusivities attributed to irradiation was much smaller than the three- to sixfold increase in

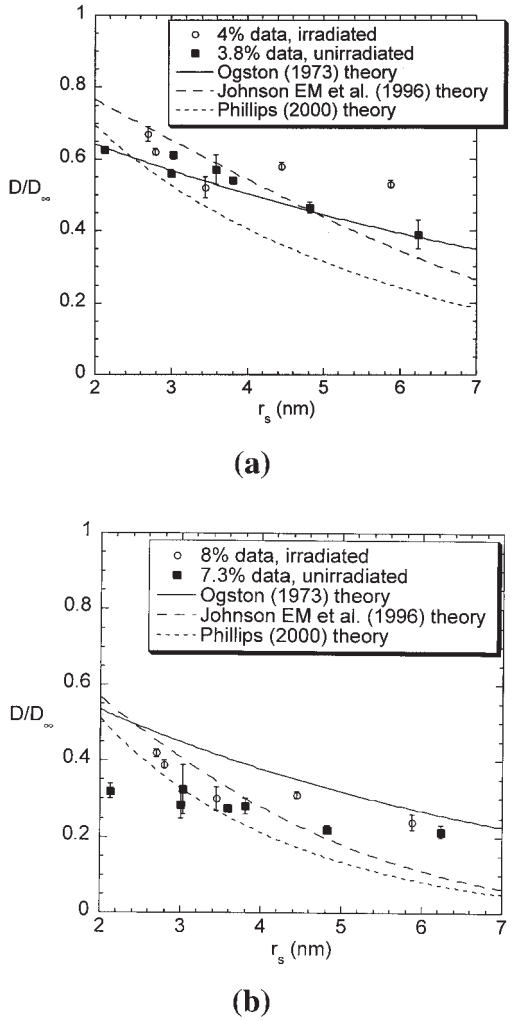

Figure 3. Relative diffusivities (D/D_∞) of proteins and Ficolls in pure agarose gels.

(a) 4.0% irradiated (present study) and 3.8% unirradiated (Johnson EM et al., 1996). (b) 8.0% irradiated (present study) and 7.3% unirradiated (Johnson EM et al., 1996). The curves are theoretical predictions based on the models of Ogston (1973), Eq. 7; Johnson EM et al. (1996), Eqs. 8–10; and Phillips et al. (2000), Eqs. 8, 9, and 11. See text for parameter values used in models.

Table 3. Relative Diffusivities (D/D_∞) in Gels*

Molecule	A	B	C	D	E	F
Ovalbumin	0.62 ± 0.01	0.53 ± 0.01	0.37 ± 0.01	0.39 ± 0.01	0.33 ± 0.02	0.19 ± 0.00
BSA	0.52 ± 0.03	0.43 ± 0.02	0.27 ± 0.03	0.30 ± 0.03	0.26 ± 0.03	0.11 ± 0.02
Ficoll 21K	0.67 ± 0.02	0.56 ± 0.02	0.46 ± 0.01	0.42 ± 0.01	0.34 ± 0.01	0.24 ± 0.01
Ficoll 61K	0.58 ± 0.01	0.47 ± 0.03	0.31 ± 0.01	0.31 ± 0.01	0.22 ± 0.01	0.12 ± 0.00
Ficoll 105K	0.53 ± 0.01	0.41 ± 0.03	0.27 ± 0.01	0.24 ± 0.02	0.15 ± 0.00	0.08 ± 0.00
DTAF	0.74 ± 0.02	0.66 ± 0.02	0.54 ± 0.01	0.59 ± 0.01	0.53 ± 0.00	0.34 ± 0.00

*The compositions of gel types A–F are shown in Table 2. Except for BSA, D/D_∞ is given as mean ± standard error for three to eight samples. For BSA, mean D/D_∞ and the corresponding error bars were calculated from the extremes of possible dimer fractions, 0.00 and 0.16, in a manner analogous to the case of a sample size of two (see text).

Darcy permeabilities found previously (White and Deen, 2002). The curves in Figure 3, which are predictions from various models, will be discussed later.

Diffusion in agarose–dextran composites

The relative diffusivities of the proteins and Ficolls in agarose–dextran composite gels are given in Table 3, along with the results for pure agarose. Results for DTAF are also shown. The columns in Table 3 (A–F) correspond to the gel compositions in Table 2. As already shown in Figure 3 for pure agarose, D/D_∞ generally decreased as the size of the diffusing macromolecule increased, for any given gel composition. Also, for a given macromolecule and a fixed agarose concentration (ϕ_a), D/D_∞ decreased as the amount of dextran (ϕ_d) was increased. Comparing the gels with the maximum dextran concentrations with pure agarose, there was generally a two- to threefold reduction in relative diffusivity.

The precision of the relative diffusivities for BSA was reduced somewhat by the fact that the fractional fluorescence in the gels ascribed to the dimer could not be determined reliably. As with the FRAP data in free solution, a three-component fit was used to interpret the data for BSA in each gel. However, the diffusivities of BSA and its dimer were too similar to use the dimer fraction in the gel samples as a fitting parameter. Accordingly, the fractional fluorescence arising from the dimer was varied from 0 (corresponding to complete exclusion of dimer from the gel) to 0.16 (corresponding to equal partition coefficients of all three components). The lower amounts of dimer led to lower bounds for the relative diffusivity of BSA, whereas the higher amounts led to upper bounds; the mean values are shown in Table 3. There was less than a 10% difference between the lower and upper bounds.

Darcy permeability

Figure 4 shows the Darcy permeability as a function of the dextran volume fraction in the gel, for both 4.0 and 8.0% agarose. The present results (open symbols) are compared with those obtained previously in gels prepared in the same way (filled symbols) (White and Deen, 2002). In both cases, the data in Table 2 were used to relate C_0 to ϕ_d. (As already mentioned, the higher dextran volume fractions estimated previously are likely to be less reliable than those in Table 2.) For both agarose concentrations, κ decreased by an order of magnitude as the dextran concentration was increased from zero to its maximum value. The present results were very similar to those found previously, as shown. The curves are stretched exponential fits to all the data at each agarose concentration. For either agarose concentration, relatively little dextran was required to produce a significant reduction in κ. That is, Figure 4 shows that incorporating $\leq$1% dextran (by volume) in either agarose gel had a greater effect on κ than did changing the agarose concentration from 4.0 to 8.0%.

Discussion

Our principal finding was that the covalent binding of modest amounts of dextran to agarose resulted in up to two- to threefold reductions in the diffusivities of proteins and Ficolls, with respect to values in pure agarose gels. The reductions in diffusivity resulting from dextran incorporation were much less than those in the Darcy permeability, which decreased by up to 10-fold, as reported before (White and Deen, 2002). We focus now on the extent to which the results can be explained by available theories for hindered diffusion in fibrous media.

The diffusivities in pure agarose were compared with predictions from three models. One approach is that of Ogston (1973), who focused on the probability that a molecule of radius r_s can complete a step through a randomly oriented array of fibers of negligible thickness. When applied to a dimensionless fiber radius $\lambda = r_f/r_s$, and fiber volume fraction ϕ, the predicted relative diffusivity is

$$\frac{D}{D_\infty} = \exp\left[-\left(\frac{1}{\lambda}+1\right)\sqrt{\phi}\right] \tag{7}$$

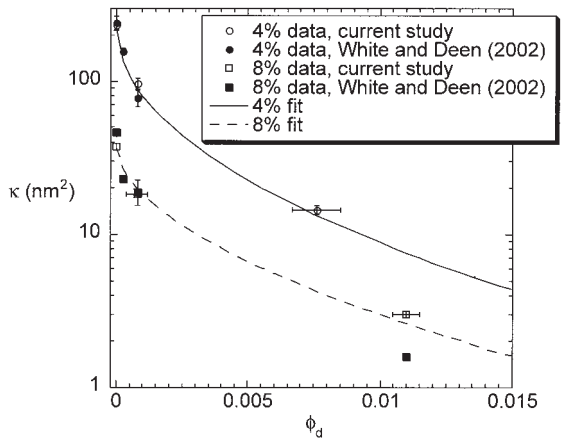

Figure 4. Darcy permeability (κ) of agarose and agarose–dextran composite gels.

The present data are compared with those of White and Deen (2002). The curves are stretched exponential fits to the data in the form of Eq. 11a, where $F = \kappa/\kappa_a$ and κ_a is the value for pure agarose. For 4% agarose, $a = 31.2$ and $b = 0.49$; for 8% agarose, $a = 31.7$ and $b = 0.55$.

In contrast to Eq. 7, where hydrodynamic effects on mobility are not considered, are two other results that combine both steric and hydrodynamic effects, ascribed to E. M. Johnson et al. (1996) and Phillips (2000), respectively. Both are based on the suggestion of Brady (1994) that the relative diffusivity be written as a product of a steric factor (S) and a hydrodynamic factor (F)

$$\frac{D}{D_\infty} = SF \tag{8}$$

The steric factor, which is similar to an inverse tortuosity, is the relative diffusivity in the absence of hydrodynamic interactions between the fibers and the macromolecular solute. That is, it describes the effect of excluding the center of a spherical solute molecule from a region of radius $r_f + r_s$ centered on any fiber. For randomly oriented arrays of fibers, the Brownian dynamics simulations of Johansson and Lofroth (1993) gave

$$S(f) = \exp(-0.84f^{1.09}) \qquad f = \left(1 + \frac{1}{\lambda}\right)\phi \tag{9}$$

This result was used by both E. M. Johnson et al. (1996) and Phillips (2000), whose models differ only in the evaluation of F. E. M. Johnson et al. (1996) based the hydrodynamic term on the drag experienced by a sphere moving through a medium described by Brinkman's equation (Brinkman, 1947), as suggested in Phillips et al. (1989). Correcting an error in one of the coefficients, pointed out in Solomentsev and Anderson (1996), yielded

$$F\left(\frac{r_s}{\sqrt{\kappa}}\right) = \left[1 + \left(\frac{r_s}{\sqrt{\kappa}}\right) + \frac{1}{9}\left(\frac{r_s}{\sqrt{\kappa}}\right)^2\right]^{-1} \tag{10}$$

This expression contains no explicit structural information; the effects of the gel structure are embodied in κ. In contrast, Phillips (2000) made use of the numerical results of Clague and Phillips (1996) for the drag on a sphere moving through a random array of fibers. Those results were correlated as a stretched exponential, as follows

$$F(\phi, \lambda) = \exp(-a\phi^b) \tag{11a}$$

$$a = 3.727 - 2.460\lambda + 0.822\lambda^2 \tag{11b}$$

$$b = 0.358 + 0.366\lambda - 0.0939\lambda^2 \tag{11c}$$

The theoretical curves in Figure 3 were based on the values of ϕ_a (Table 2) and κ for agarose (Figure 4), together with a value of r_f (=1.64 nm) inferred recently from equilibrium partitioning data for untreated agarose (Lazzara and Deen, 2004). The expression of Ogston (Eq. 7) gave approximately the correct slope in the plots of relative diffusivity vs. molecular radius at either agarose concentration, although it consistently overestimated the relative diffusivities in 8.0% agarose. A tendency of Eq. 7 to greatly overestimate relative diffusivities in unirradiated agarose gels was noted previously (E. M. Johnson et al, 1996). The models of Johnson and Deen (Eqs. 8–10) and Phillips (Eqs. 8, 9, and 11) both yielded slopes that were too large. The results obtained with two other models for diffusion in gels (Amsden, 1998; Bosma et al., 2000) generally gave larger mean square errors when applied to our agarose data than did those shown in Figure 3; those curves have been omitted for clarity. Thus, none of the available theories precisely captures the behavior of macromolecular diffusivities in pure agarose.

The only one of the models discussed above that can be applied readily to the diffusivity data in the agarose–dextran composite gels is the effective medium approach of E. M. Johnson et al. (1996). That is, even if it is postulated that the composite gels can be modeled as a mixture of randomly oriented fibers of differing radii, the other approaches cannot be extended readily to incorporate a second fiber type. In testing the predictive ability of the effective medium model for composite gels, we chose to focus on the diffusivity ratio D/D_a, where D_a is the value in pure agarose. Normalizing the gel diffusivity using the value in agarose tends to separate the ability of the model to predict D_a from its ability to predict the effects of the added dextran on D. An additional assumption we made is that S in the agarose–dextran gels is determined mainly by agarose. The idea that dextran does not contribute significantly to the steric factor for diffusion is supported by the fact that relative diffusivities of globular proteins in dextran solutions have been found to be described accurately by setting $S = 1$ in Eq. 8 and evaluating F using Eq. 10 (Kosar and Phillips, 1995). It also appears that S is near unity in hyaluronic acid solutions (Phillips et al., 1989) and polyacrylamide gels (Kapur et al., 1997), suggesting that steric hindrances to diffusion may be nearly absent, in general, if the polymeric obstacles are relatively flexible. In contrast to the polymers just mentioned, agarose forms rigid fibrils that do not exhibit detectable Brownian motion (Mackie et al., 1978). With the assumption that S was determined primarily by the agarose, applying Eqs. 8 and 10 to agarose gels with and without dextran gives

$$\frac{D}{D_a} = \frac{1 + \left(\frac{r_s}{\sqrt{\kappa_a}}\right) + \frac{1}{9}\left(\frac{r_s}{\sqrt{\kappa_a}}\right)^2}{1 + \left(\frac{r_s}{\sqrt{\kappa}}\right) + \frac{1}{9}\left(\frac{r_s}{\sqrt{\kappa}}\right)^2} \tag{12}$$

where κ_a is the Darcy permeability for pure agarose and the S terms have cancelled.

Figure 5 compares the experimental diffusivity ratios with the predictions from Eq. 12. For either 4.0 or 8.0% agarose, the model underestimated the effects of dextran at the lower dextran level (that is, it overestimated D/D_a), but was quite accurate at the higher dextran level. Overall, given the simplicity of Eq. 12 and the absence of adjustable parameters, the predictions are remarkably good. The agreement between the model and data in Figure 5 supports the use of Eq. 10 for evaluating F in agarose and agarose–dextran gels. Moreover, it suggests that the limited success in predicting diffusivities in pure agarose (particularly the slopes in Figure 3), may have been attributable mainly to problems with Eq. 9. Specifically, it suggests that Eq. 9, when applied to agarose, may have too strong a dependency of S on r_s.

The expression for S in Eq. 9 was obtained from simulations

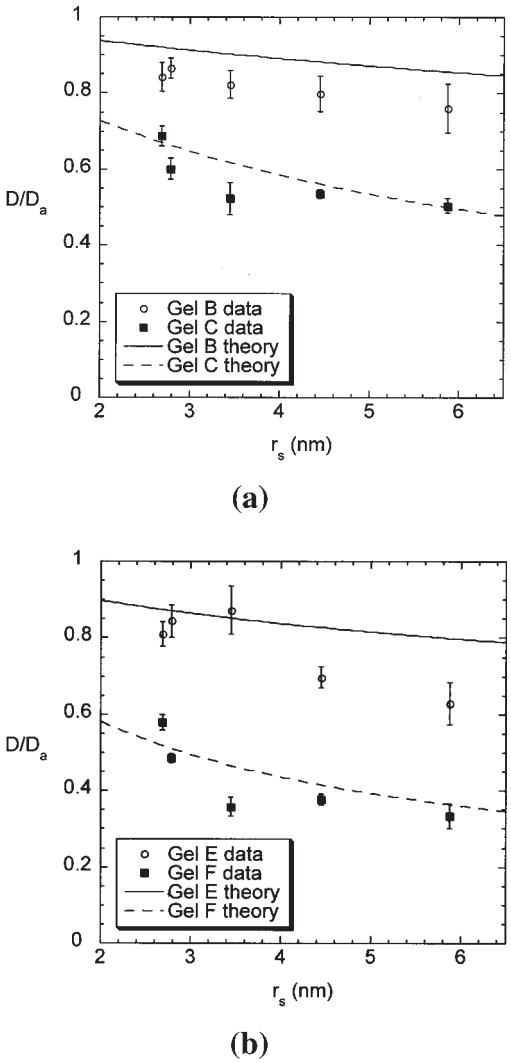

Figure 5. Diffusivities in composite gels relative to values in pure agarose.

(a) 4.0% agarose with $\phi_d = 0.0008$ (Gel B) and $\phi_d = 0.0076$ (Gel C); (b) 8.0% agarose with $\phi_d = 0.0008$ (Gel E) and $\phi_d = 0.011$ (Gel F). The theoretical curves in each case are based on Eq. 12.

based on randomly positioned and oriented fibers of uniform radius (Johansson and Lofroth, 1993). Modeling untreated agarose in this manner led to very accurate predictions of equilibrium partition coefficients for BSA and several Ficolls (Lazzara and Deen, 2004), provided that the fiber radius was chosen as 1.6 nm. That value is close to the number-average fiber radius of 1.9 nm suggested by small-angle X-ray scattering data (Djabourov et al., 1989). However, attempts to predict Darcy permeabilities for agarose from fiber matrix models have generally yielded much poorer results (Clague and Phillips, 1997; E. M. Johnson et al., 1996; Johnston and Deen, 1999; White and Deen, 2002). Complicating the situation is that electron-beam treatments alter the structural properties of agarose, as evidenced by increases in diffusivity (present data) and Darcy permeabilty (White and Deen, 2002). Thus, it is not clear at present what geometric model(s) might be adopted to improve the results for S, either for treated or untreated agarose.

One feature of the present results is that the reductions in κ after dextran incorporation into agarose were proportionately much larger than those in D/D_∞. In general, changes in the Darcy permeability of gels will not necessarily be disproportionate to those in diffusivities. For example, Kapur et al. (1996, 1997), in studies of protein diffusion and water flow through polyacrylamide gels confined in porous membranes, found moderate and comparable percentage declines in κ and D/D_∞ as the polyacrylamide volume fraction was increased from 0.044 to 0.094. For a uniform, random fiber matrix, the dependency of κ on ϕ varies approximately as $-(\ln \phi)/\phi$ (Jackson and James, 1986). Thus, at relatively high volume fractions (as in the polyacrylamide study), κ is not nearly as sensitive to ϕ as it is at low volume fractions. In the present study, where the more important volume fraction was ϕ_d, much larger changes in κ were seen because ϕ_d was much smaller.

In general, protein diffusivities may depend on pH, ionic strength, and protein concentration (Raj and Flygare, 1974). From pH 10.5 to about 5, BSA has a compact configuration, with a negative charge that diminishes as the isoelectric pH of 4.8 is approached. At still lower pH values (<4.8), BSA acquires a net positive charge and undergoes a conformational change to a more expanded form. Raj and Flygare (1974) found that for BSA concentrations of 1–2% by weight and with pH between 6 and 7, the diffusivity was independent of pH, concentration, and ionic strength (within the range 0.01–0.50 M). Thus, the present results, which were obtained using dilute solutions at pH 7 and an ionic strength of 0.1 M, should have been insensitive to those factors. Moreover, because agarose and dextran are essentially neutral, no additional charge effects (beyond the intramolecular forces that influence the BSA conformation) are expected to have been present.

Conclusion

In summary, the reductions in macromolecular diffusivities caused by incorporating various amounts of dextran into agarose gels could be predicted fairly accurately from the measured decreases in Darcy permeability, using an effective medium model. This suggests that one might be able to predict diffusivity variations in complex, multicomponent hydrogels (such as those in body tissues) in the same manner, provided that values of κ can be obtained. Until more detailed structure-based models can be developed, ones that include multiple types of (possibly flexible) fibers, the effective medium approach seems to provide an attractive alternative for modeling diffusion in complex hydrogels.

Notation

a = parameter in stretched exponential function, Eq. 11
A = exposed membrane area
b = parameter in stretched exponential function, Eq. 11
C_0 = dextran concentration in initial equilibration solution used in membrane preparation
C_t = dextran concentration in final equilibration solution for irradiated (treated) gels
C_u = dextran concentration in final equilibration solution for unirradiated (untreated) gels
D = diffusivity in gel
D_a = diffusivity in pure agarose gel
D_i = diffusivity of species i in Eq. 6
D_∞ = diffusivity in free solution

f = adjusted volume fraction, Eq. 9
$f(t)$ = dimensionless Fourier-transformed fluorescence intensity in Eq. 6
F = hydrodynamic hindrance factor for diffusion, Eq. 8
$\tilde{I}$ = Fourier-transformed fluorescence intensity, Eq. 6
k_B = Boltzmann's constant
M_N = number-average molecular weight
M_W = weight-average molecular weight
ΔP = transmembrane pressure drop in hydraulic permeability measurements
Q = volumetric flow rate in hydraulic permeability measurements
r_f = fiber radius
r_s = Stokes–Einstein radius, Eq. 5
S = steric hindrance factor for diffusion, Eq. 8
t = time
T = absolute temperature
u, v = spatial frequencies in Fourier-transformed images, Eq. 6
V_0 = volume of initial and final equilibration solutions
$\hat{V}_d$ = specific volume of dextran
V_g = gel volume
x_i = fraction of fluorescence signal attributed to species i, Eq. 6

Greek letters

β = correction factor for flow resistance attributed to the polyester mesh support, Eq. 4
δ = gel thickness
ϕ = fiber volume fraction, total
ϕ_a = agarose volume fraction
ϕ_d = dextran volume fraction
Φ = equilibrium partition coefficient, gel concentration divided by free solution concentration
η = dextran immobilization fraction, Eq. 2
κ = Darcy permeability
κ_a = Darcy permeability of pure agarose gel
λ = dimensionless fiber radius, r_f/r_s
μ = viscosity of water

Acknowledgments

This work was supported by Grant DK 20368 from the National Institutes of Health. Professor T. Alan Hatton kindly allowed us full use of several major pieces of equipment that were used to build the FRAP apparatus. Kenneth Wright provided essential assistance in the electron beam irradiation of the gels. Christiana Obiaya assisted with the Darcy permeability measurements.

Literature Cited

Amsden, B., "Solute Diffusion within Hydrogels. Mechanisms and Models," *Macromolecules*, **31**, 8382 (1998).
Berk, D. A., F. Yuan, M. Leunig, and R. K. Jain, "Fluorescence Photobleaching with Spatial Fourier Analysis: Measurement of Diffusion in Light-Scattering Media," *Biophys. J.*, **65**, 2428 (1993).
Bohrer, M. P., W. M. Deen, C. R. Robertson, J. L. Troy, and B. M. Brenner, "Influence of Molecular Configuration on the Passage of Macromolecules across the Glomerular Capillary Wall," *J. Gen. Physiol.*, **74**, 583 (1979).
Bolton, G. R., W. M., Deen, and B. S. Daniels, "Assessment of the Charge-Selectivity of Glomerular Basement Membrane using Ficoll Sulfate," *Am. J. Physiol. Renal Physiol.*, **274**, F889 (1998).
Bosma, J. C., and J. A. Wesselingh, "Partitioning and Diffusion of Large Molecules in Fibrous Structures," *J. Chromatogr. B.*, **743**, 169 (2000).
Brady, J., "Hindered Diffusion," Extended Abstracts, AIChE Annual Meeting, San Francisco, CA, p. 320 (1994).
Brinkman, H. C., "A Calculation of the Viscous Force Exerted by a Flowing Fluid in a Dense Swarm of Particles," *Appl. Sci. Res A*, **1**, 27 (1947).
Burczak, K., T. Fujisato, M. Hatada, and Y. Ikada, "Protein Permeation through Poly(vinyl alcohol) Hydrogel Membranes," *Biomaterials*, **15**, 231 (1994).
Clague, D. S., B. D. Kandhai, R. Zhang, and P. M. A. Sloot. "Hydraulic Permeability of (Un)Bounded Fibrous Media Using the Lattice Boltzmann Method," *Phys. Rev. E*, **61**, 616 (2000).
Clague, D. S., and R. J. Phillips, "Hindered Diffusion of Spherical Macromolecules through Dilute Fibrous Media," *Phys. Fluids*, **8**, 1720 (1996).
Clague, D. S., and R. J. Phillips, "A Numerical Calculation of the Hydraulic Permeability of Three-Dimensional Disordered Fibrous Media," *Phys. Fluids*, **9**, 1562 (1997).
De Belder, A. N., and K. Granath, "Preparation and Properties of Fluorescein-Labeled Dextrans," *Carbohydr. Res.*, **30**, 375 (1973).
Deen, W. M., "Hindered Transport of Large Molecules in Liquid-Filled Pores," *AIChE J.*, **33**, 1409 (1987).
Djabourov, M., A. H. Clark, D. W. Rowland, and S. B. Ross-Murphy, "Small-Angle X-ray-Scattering Characterization of Agarose Sols and Gels," *Macromolecules*, **22**, 180 (1989).
Dubois, M., K. A. Gilles, J. K. Hamilton, P. A. Rebers, and F. Smith, "Colorimetric Method for Determination of Sugars and Related Substances," *Anal. Chem.*, **28**, 350 (1956).
Gibbs, S. J., E. N. Lightfoot, and T. W. Root, "Protein Diffusion in Porous Gel Filtration Chromatography Media Studied by Pulsed Field Gradient NMR Spectroscopy," *J. Phys. Chem.*, **96**, 7458 (1992).
Gong, J. P., N. Hirota, A. Kakugo, T. Narita, and Y. Osada, "Effect of Aspect Ratio on Protein Diffusion in Hydrogels," *J. Phys. Chem. B*, **104**, 9904 (2000).
Hou, L., F. Lanni, and K. Luby-Phelps, "Tracer Diffusion in F-Actin and Ficoll Mixtures: Toward a Model for Cytoplasm," *Biophys. J.*, **58**, 31 (1990).
Jackson, G. W., and D. F. James, "The Permeability of Fibrous Porous Media," *Can. J. Chem. Eng.*, **64**, 362 (1986).
Jain, R. K., R. J. Stock, S. R. Chary, and M. Rueter, "Convection and Diffusion Measurements Using Fluorescence Recovery after Photobleaching and Video Image Analysis: In Vitro Calibration and Assessment," *Microvasc. Res.*, **39**, 77 (1990).
Johansson, L., and J. E. Lofroth, "Diffusion and Interaction in Gels and Solutions. 4. Hard Sphere Brownian Dynamics Simulations," *J. Chem. Phys.*, **98**, 7471 (1993).
Johnson, E. M., D. A. Berk, R. K. Jain, and W. M. Deen, "Diffusion and Partitioning of Proteins in Charged Agarose Gels," *Biophys. J.*, **68**, 1561 (1995).
Johnson, E. M., D. A. Berk, R. K. Jain, and W. M. Deen, "Hindered Diffusion in Agarose Gels: Test of the Effective Medium Model," *Biophys. J.*, **70**, 1017 (1996).
Johnson, E. M., and W. M. Deen, "Hydraulic Permeability of Agarose Gels," *AIChE J.*, **42**, 1220 (1996).
Johnson, M. E., D. A. Berk, D. Blankschtein, D. E. Golan, R. K. Jain, and R. S. Langer, "Lateral Diffusion of Small Compound in Human Stratum Corneum and Model Lipid Bilayer Systems," *Biophys. J.*, **71**, 2656 (1996).
Johnston, S. T., and W. M. Deen, "Hindered Convection of Proteins in Agarose Gels," *J. Membr. Sci.*, **153**, 271 (1999).
Kapur, V., J. Charkoudian, and J. L. Anderson, "Transport of Proteins through Gel-Filled Porous Membranes," *J. Membr. Sci.*, **131**, 143 (1997).
Kapur, V., J. C. Charkoudian, S. B. Kessler, and J. L. Anderson, "Hydrodynamic Permeability of Hydrogels Stabilized within Porous Membranes," *Ind. Eng. Chem. Res.*, **35**, 3179 (1996).
Key, P. Y., and D. B. Sellen, "A Laser Light-Scattering Study of the Structure of Agarose Gels," *J. Polym. Sci. Polym. Phys. Ed.*, **20**, 659 (1982).
Kosar, T. F., and R. J. Phillips, "Measurement of Protein Diffusion in Dextran Solutions by Holographic Interferometery," *AIChE J.*, **41**, 701 (1995).
Larson, R. J., and M. L. Marx, *An Introduction to Mathematical Statistics and Its Applications*, 2nd Edition, Prentice-Hall, Englewood Cliffs, NJ (1986).
Lazzara, M. J., and W. M. Deen, "Effects of Concentration on the Partitioning of Macromolecule Mixtures in Agarose Gels," *J. Colloid Interface Sci.*, **272**, 288 (2004).
Mackie, W., D. B. Sellen, and J. Sutcliffe, "Spectral Broadening of Light Scattered from Polysaccharide Gels," *Polymer*, **19**, 9 (1978).
Moussaoui, M., M. Benlyas, and P. Wahl, "Diffusion of Proteins in Sepharose Cl-B Gels," *J Chromatogr.*, **591**, 115 (1992).
Ogston, A. G., B. N. Preston, and J. D. Wells, "On the Transport of Compact Particles through Solutions of Chain Polymers," *Proc. R. Soc. Lond. A*, **333**, 297 (1973).
Oliver, J. D., S. Anderson, J. L. Troy, B. M. Brenner, and W. M. Deen,

"Determination of Glomerular Size-Selectivity in the Normal Rat with Ficoll," *J. Am. Soc. Nephrol.*, **3**, 214 (1992).
Phillips, R. J., "A Hydrodynamic Model for Hindered Diffusion of Proteins and Micelles in Hydrogels," *Biophys. J.*, **79**, 2250 (2000).
Phillips, R. J., W. M. Deen, and J. F. Brady, "Hindered Transport of Spherical Macromolecules in Fibrous Membranes and Gels," *AIChE J.*, **35**, 1761 (1989).
Phillips, R. J., W. M. Deen, and J. F. Brady, "Hindered Transport in Fibrous Membranes and Gels: Effect of Solute Size and Fiber Configuration," *J. Colloid Interface Sci.*, **139**, 363 (1990).
Pluen, A., P. A. Netti, R. K. Jain, and D. A. Berk, "Diffusion of Macromolecules in Agarose Gels: Comparison of Linear and Globular Configurations," *Biophys. J.*, **77**, 542 (1999).
Putnam, F. W., *The Plasma Proteins: Structure, Function, and Genetic Control*, 2nd Edition, Vol. 1, p. 62, Academic Press, New York (1975).
Raj, T., and W. H. Flygare, "Diffusion Studies of Bovine Serum Albumin by Quasielastic Light Scattering," *Biochemistry*, **13**, 3336 (1974).
Saltzman, W. M., M. L. Radomsky, K. J. Whaley, and R. A. Cone, "Antibody Diffusion in Human Cervical Mucus," *Biophys. J.*, **66**, 508 (1994).
Solomentsev, Y. E., and J. L. Anderson, "Rotation of a Sphere in Brinkman Fluids," *Phys. Fluids*, **8**, 1119 (1996).
Tsay, T. T., and K. A. Jacobson, "Spatial Fourier Analysis of Video Photobleaching Measurements: Principles and Optimization," *Biophys. J.*, **60**, 360 (1991).
Wattenbarger, M. R., V. A. Bloomfield, Z. Bu, and P. S. Russo, "Tracer Diffusion of Proteins in DNA Solutions," *Macromolecules*, **25**, 5263 (1992).
White, J. A., and W. M. Deen, "Effects of Solute Concentration on Equilibrium Partitioning of Flexible Macromolecules in Fibrous Membranes and Gels," *Macromolecules*, **34**, 8278 (2001).
White, J. A., and W. M. Deen, "Agarose–Dextran Gels as Synthetic Analogs of Glomerular Basement Membrane: Water Permeability," *Biophys. J.*, **82**, 2081 (2002).
Zhang, X. M., N. Hirota, T. Narita, J. P. Gong, Y. Osada, and K. S. Chen, "Investigation of Molecular Diffusion in Hydrogel by Electronic Speckle Pattern Interferometery," *J. Phys. Chem. B*, **103**, 6060 (1999).

Manuscript received Dec. 5, 2003, and revision received Feb. 20, 2004.